Dynamic Structures of Intact Chicken Erythrocyte Chromatins as Studied by ^1H-^{31}P Cross-Polarization NMR

Hideo Akutsu, Shozoh Nishimoto, and Yoshimasa Kyogoku

Department of Bioengineering, Faculty of Engineering, Yokohama National University, Hodogaya-ku, Yokohama 240, and Institute for Protein Research, Osaka University, Suita, Osaka 565 Japan

ABSTRACT The dynamic properties of DNA in intact chicken erythrocyte cells, nuclei, nondigested chromatins, digested soluble chromatins, H1, H5-depleted soluble chromatins and nucleosome cores were investigated by means of single-pulse and ^1H-^{31}P cross-polarization NMR. The temperature dependence of the phosphorus chemical shift anisotropy was identical for the former three in the presence of 3 mM $MgCl_2$, suggesting that the local higher order structure is identical for these chromatins. The intrinsic phosphorus chemical shift anisotropy of the nucleosome cores was −159 ppm. The chemical shift anisotropy of DNA in the chromatins can be further averaged by the motion of the linker DNA. The spin-lattice relaxation time in the rotating frame of the proton spins ($T_{1\rho}$) of the nondigested chromatins was measured at various locking fields. The result was analyzed on the assumption of the isotropic motion to get a rough value of the correlation time of the motion efficient for the relaxation, which was eventually ascribed to the segmental motion of the linker DNA with restricted amplitude. The 30 nm filament structure induced by NaCl was shown to be dynamically different from that induced by $MgCl_2$. Side-by-side compaction of 30-nm filaments was suggested to be induced in the $MgCl_2$ concentration range higher than 0.3 mM. Biological significance of the dynamic structure was discussed in connection with the results obtained.

INTRODUCTION

Eukaryotic chromosomes are known to have an organized and compact structure. The phenomena of decondensation and condensation of chromatins are very important in transcription and replication. Extensive studies have been carried out to elucidate the condensation of chromatins (van Holde, 1989). Most basic folding of DNA occurs in the nucleosome cores, where the DNA is wrapped around an octamer of the core histone proteins (H2A, H2B, H3, and H4) (Richmond et al., 1984). Nucleosome cores and linker DNA comprise the so-called 10-nm filament in the presence of the fifth histone, H1 (or H5). Crystal structure of the globular domain of H5 histone was established, and a model for the binding with the nucleosomal DNA was proposed (Ramakrishnan et al., 1993). An electron microscopic study of nuclease-digested chromatins (soluble chromatins) showed that they undergo further compaction, from 10- to 30-nm filaments, depending on the salt concentration (Finch and Klug, 1976). For the 30-nm filament, there are three major types of models, namely, solenoid models (Finch and Klug, 1976; McGhee et al., 1983; Butler, 1984), twisted-ribbon models (Worcel et al., 1981; Woodcock et al., 1984), and cross-linker models (Staynov, 1983; Makarov et al., 1985; Williams et al., 1986; Bordas et al., 1986; Williams and Langmore, 1991). Although the solenoid models are now widely accepted, controversy regarding the higher order structures remains (van Holde, 1989). Recently, biological roles of the chromatins have been elucidated in terms of molecular structure. For example, histones H1 and H5 have turned out to be repressors of transcription (Hayes and Wolffe, 1992). Actually, the structures of the globular domain of H5 are very similar to those of catabolite-activating protein (CAP) (Ramakrishnan et al., 1993).

To get more direct evidence for the biological significance of the higher order structures, it is desirable to investigate them in vivo or in a system close to it. A few works on in vivo systems have been carried out to substantiate the results on digested (soluble) chromatins. Low angle x-ray diffraction of intact chicken erythrocytes or sea urchin sperm gave broad 40-nm reflections, which were ascribed to side-by-side packing of chromatin fibers (Langmore and Paulson, 1983; Widom et al., 1985). The fluorescence anisotropy decay showed that the rigidity of the linker DNA in the chicken erythrocyte nuclei is similar to that in the 30-nm filaments of digested (soluble) chromatins (Ashikawa et al., 1985). We have shown the presence of the 30-nm filament structure in intact chicken erythrocytes by means of ^1H-^{31}P cross-polarization NMR (Nishimoto et al., 1987). A polarized photobleaching study has been carried out on the intact nuclei of mudpuppy and sea urchin, which provided information on the dynamics of these higher order structures (Selvin et al., 1990). Because the nucleosome itself can be turned to a transcription site by biological modifications (van Holde, 1993), elucidation of the dynamic structures of intact chromatins will shed light on the mechanism of the transcriptional and replicational activities in the nuclei as discussed by Hansen and Ausio (1992). To approach this goal, we here extend our previous work and report the detailed dynamic properties of chicken erythrocyte chromatins in intact systems.

Received for publication 15 December 1993 and in final form 22 April 1994

Address reprint requests to Hideo Akutsu, Department of Bioengineering, Faculty of Engineering, Yokohama National University, Tokiwadai-156, Hodogaya-ku, Yokohama 240 Japan. Tel.: 011-81-45-335-1451; Fax: 011-81-45-331-6143.

0006-3495/94/08/804/08 $2.00

MATERIALS AND METHODS

Erythrocytes were obtained from chicken blood diluted with an approximately equal volume of SSC buffer (150 mM NaCl, 15 mM sodium citrate), followed by centrifugation at 4000 × *g* for 15 min. Erythrocyte nuclei, chromatins, and nucleosome cores were prepared according to Ashikawa et al. (1985). Nondigested chromatins were obtained as follows. Nuclear envelopes were ruptured by gently suspending chicken erythrocyte nuclei in a large volume of TE buffer (1 mM Tris, 0.2 mM EDTA, pH7.4). Then 1 M NaCl was added dropwise and gently to a final concentration of 100 mM. The aggregated chromatins were pelleted by centrifugation at 4,000 × *g* for 15 min. To obtain digested soluble chromatins, the nuclei (A_{260} = 50 in 1 N NaOH) were incubated for 5 min at 37°C in the presence of 40 units/ml micrococcal nuclease, 1 mM $CaCl_2$ and 1 mM phenylmethanesulfonyl fluoride (PMSF). The reaction was terminated by adding EDTA (final, 5 mM) and putting the reaction mixture in ice. The digested nuclei were suspended in 1 mM Tris, 1 mM EDTA, pH7.4, and then the mixture was centrifuged at 10,000 × *g* for 20 min. The supernatant fraction was used as the digested (soluble) chromatins. Removal of histones H1 and H5 was performed by ultracentrifugation of the digested chromatins in 0.65 M NaCl, 10 mM Tris, 0.2 mM EDTA, 0.5 mM PMSF, pH 7.5 (100,000 × *g*, 15 h) over a cushion of several milliliters of 30% sucrose containing 0.65 M NaCl, 10 mM Tris, pH 7.5. The chromatin fraction was subjected to the same ultracentrifugation again. The fraction obtained is referred to as the H1,H5-depleted chromatins. To prevent nucleosome rearrangement in the H1,H5-depleted chromatin, the sample was always kept at 2–4°C. To determine whether nucleosome rearrangement had occurred in the H1,H5-depleted chromatins, the sample was digested with micrococcal nuclease, and the nuclease cutting pattern of the extracted DNA in the digested sample was checked by polyacrylamide gel electrophoresis. Nucleosome cores were obtained as follows. The buffer of the H1,H5-depleted chromatin solution was replaced by 20 mM ammonium acetate, 5 mM Tris, pH 7.8 through dialysis. Then the solution was diluted to A_{260} = 50. The chromatin was digested with micrococcal nuclease (100 units/ml) in the presence of 1 mM $CaCl_2$ and 0.25 mM PMSF at 37°C for about 6 min. After stopping the reaction, the reaction mixture was applied on a sucrose gradient (5–20%), followed by ultracentrifugation at 121,700 × *g* for 24 h. Then the nucleosome core fraction was collected. The length of the DNA was confirmed to be about 145 base pairs by polyacrylamide gel electrophoresis. The proteins in all samples were checked by SDS-polyacrylamide gel electrophoresis as described by Laemmli (1970).

Sample preparations for NMR measurements were obtained as follows. In the case of nuclei and nondigested chromatins, the pellet was dialyzed against STM buffer (10 mM NaCl, 10 mM Tris, 3.0 mM $MgCl_2$, pH 7.4) containing 30% sucrose or TE buffer containing 30% sucrose and the indicated salt. A sample in dialysis tubing was immersed in the same buffer solution in a 10 mmϕ NMR tube and used for NMR measurements. The digested chromatins, H1,H5-depleted chromatins, and nucleosome cores were ultracentrifuged at 60,000 rpm (Beckman, type 65 rotor) for 17 h in the presence of several milliliters of a 5% sucrose cushion containing the same buffer. The pellet was used for the NMR measurements. ^{31}P NMR spectra were obtained at 40.3 MHz with a JEOL FX-100 NMR spectrometer equipped with a solid-state NMR system. The field was locked on external deuterium oxide. A probe head specially designed for high-power and variable temperature measurements was used, in which the sample tube was held vertically. A 45° pulse (typically 3–4 μs) and a 3.0- or 3.6 s relaxation delay was used for the single-pulse measurements. The same relaxation delay was used for the cross-polarization sequence. The cross-polarization pulse sequence used was reported previously (Akutsu, 1986). For the $T_{1\rho}$ measurements, a delay time was inserted between the 90° pulse of protons and the start of the thermal contact (Stejskal et al., 1981; Akutsu, 1986). The proton spins were irradiated during data acquisition. The decoupling power was 40–50 kHz except for experiments on the field dependence of $T_{1\rho}$. Temperature calibration for the thermal contact and proton-decoupling was carried out. The number of data points used for a spectral width of 50,000 Hz was 4096. Phosphoric acid (85%) was used as an external standard. An exponential window function with a 100 Hz broadening factor was used.

RESULTS

Phosphorus NMR spectra of chicken erythrocyte cells, nuclei, and nondigested chromatins

A phosphorus NMR spectrum of chicken erythrocyte nuclei in STM buffer at 4°C was obtained by single pulse and is presented at the bottom of Fig. 1. Because 91.2% of the phosphorus in a nucleus is located in DNA (Zentgraf et al., 1971), this spectrum represents the DNA in the nuclei. This is a typical asymmetric powder pattern, which is characteristic for phosphorus under restricted motions. When the sample was incubated at 90°C for 25 min, it gave a symmetric pattern as shown on the top of Fig. 1. This shows that heat denaturation of proteins in the nuclei (Cavazza et al., 1991) induces a drastic change in the motion of DNA. The chemical shift anisotropy ($\Delta\sigma = \sigma_{11} - \sigma_{33}$; σ_{11}, σ_{22} and σ_{33} are the principal components of the residual chemical shift tensor) of the asymmetric powder pattern of DNA in the nuclei is plotted as a function of temperature in Fig. 2. We have reported that the nuclei in intact chicken erythrocyte cells and the nondigested chromatins in STM buffer gave similar powder patterns (Nishimoto et al., 1987). By use of the ^1H-^{31}P cross-polarization method, the spectrum of the DNA in intact chicken erythrocyte cells could be selectively obtained. The ^{31}P-NMR spectrum of the DNA in the intact erythrocytes was measured at a variety of temperatures in this work. The

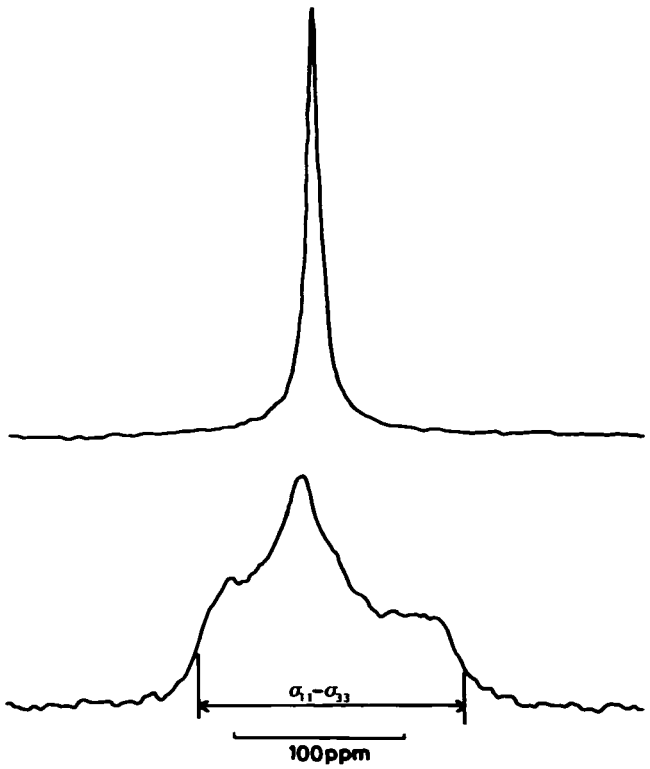

FIGURE 1 ^{31}P-NMR spectra of chicken erythrocyte nuclei measured by single pulse. (*Bottom*) Intact nuclei at 4°C; (*top*) nuclei at 40°C after incubation at 90°C for 25 min. The phosphorus chemical shift anisotropy ($\sigma_{11} - \sigma_{33}$) is indicated in the bottom spectrum.

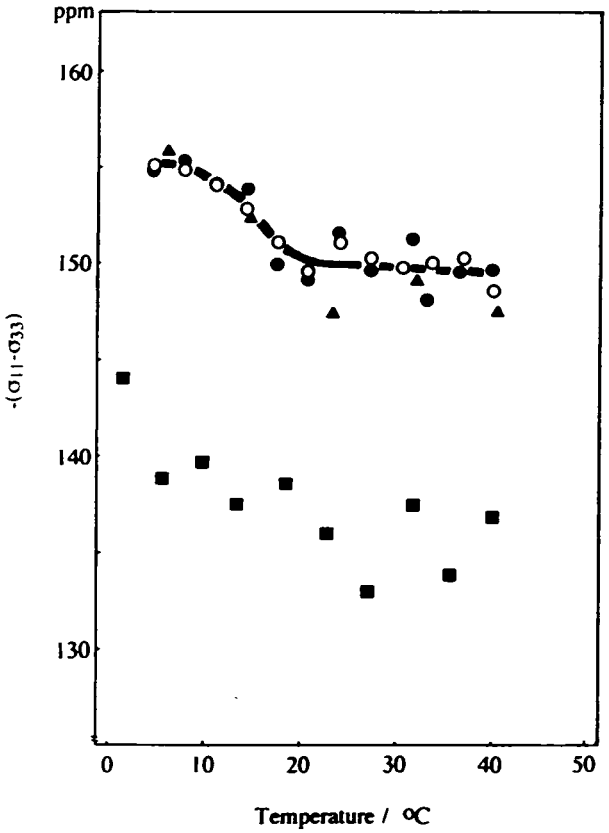

FIGURE 2 Temperature dependence of the phosphorus chemical shift anisotropies of the chromatins up to 40°C. (▲) Intact chicken erythrocyte cells; (○) intact nuclei in STM buffer; (●) nondigested chromatins in STM buffer; (■) nondigested chromatins in TE buffer. STM buffer; 10 mM NaCl, 10 mM Tris, 3 mM $MgCl_2$, pH7.4. TE buffer; 1 mM Tris, 0.2 mM EDTA, pH 7.4.

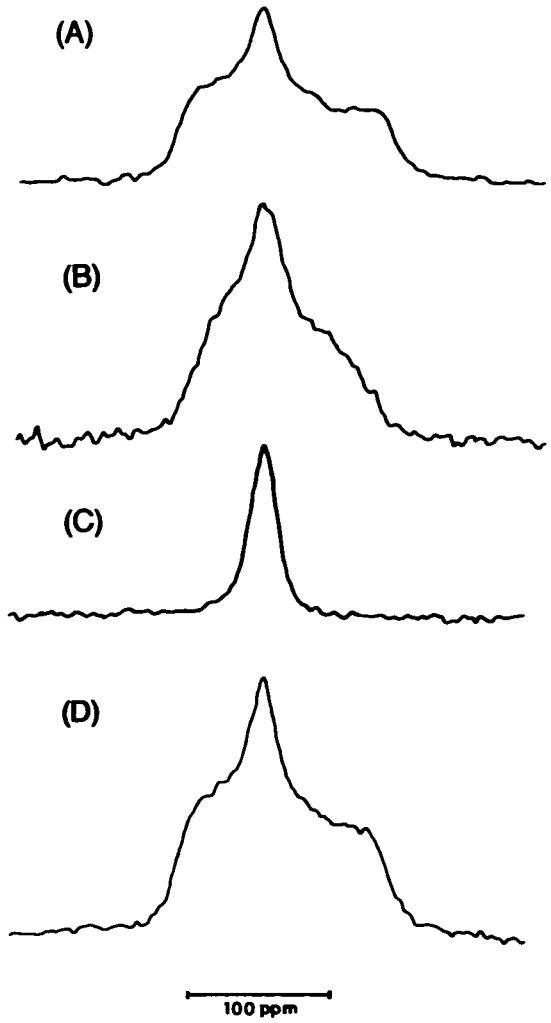

FIGURE 3 ^{31}P-NMR spectra of nondigested chromatins obtained by single pulse at 4°C in the presence of 3.0 mM $MgCl_2$ (*A*), 0 mM $MgCl_2$ (*B*), or 3.0 M NaCl (*C*) in TE buffer. (*D*) Spectrum of nucleosome cores in TE buffer obtained by cross-polarization.

chemical shift anisotropies are presented in Fig. 2 along with those of the nuclei and nondigested chromatins. Although the values for intact cells at temperatures higher than 20°C are a little smaller than others, most of them fall on the same curve. This shows that the higher order structure of the nondigested chromatins in STM buffer is essentially the same as that of the chromatins in the nuclei and intact cells. This powder pattern was ascribed to the 30-nm filament (Nishimoto et al., 1987). The chemical shift anisotropy changed inbetween 5 and 20°C, suggesting that a transition in the motional state took place in this temperature range.

The powder patterns of the nondigested chromatins in the STM and TE buffers are presented in Fig. 3, *A* and *B*, respectively. As can be seen in Fig. 3 *B*, the chemical shift anisotropy was further averaged in TE buffer. The chemical shift anisotropy is presented in Fig. 2 at a variety of temperatures. To confirm that the residual chemical shift anisotropy of the nondigested chromatins in TE buffer is caused by the interaction between DNA and histone proteins, the chromatins were dialyzed against 3.0 M NaCl and then the spectra were measured in the presence of 3.0 M NaCl. Most histone proteins become detached from the DNA in the presence of 3.0 M NaCl (van Holde, 1989). As shown in Fig. 3 *C*, a symmetric signal was obtained at 4°C. This clearly shows that when the specific interactions between the histone proteins and DNA are destroyed, the motion of DNA is drastically enhanced and the DNA does not give an asymmetric powder pattern anymore.

The ratio of the cross-polarization and single-pulse intensities was examined at 4°C as a measure of the cross-polarization efficiency. It was plotted as a function of the magnesium chloride or sodium chloride concentration in Fig. 4. Cross-polarization and single-pulse spectra were obtained for the same sample and at the same time. The intensity of a cross-polarization spectrum is quite sensitive to the sample conditions. Because we used a vertical coil and a vertical sample tube, the sample conditions could be kept stable for a long time. In the presence of $MgCl_2$, the intensity ratio increased from 1.2 to 1.9 in the range of 0.1 to 1.0 mM $MgCl_2$. However, the change in chemical shift anisotropy took place in the range of 0.1–0.3 mM $MgCl_2$ (Nishimoto et al., 1987). This concentration range is in good agreement

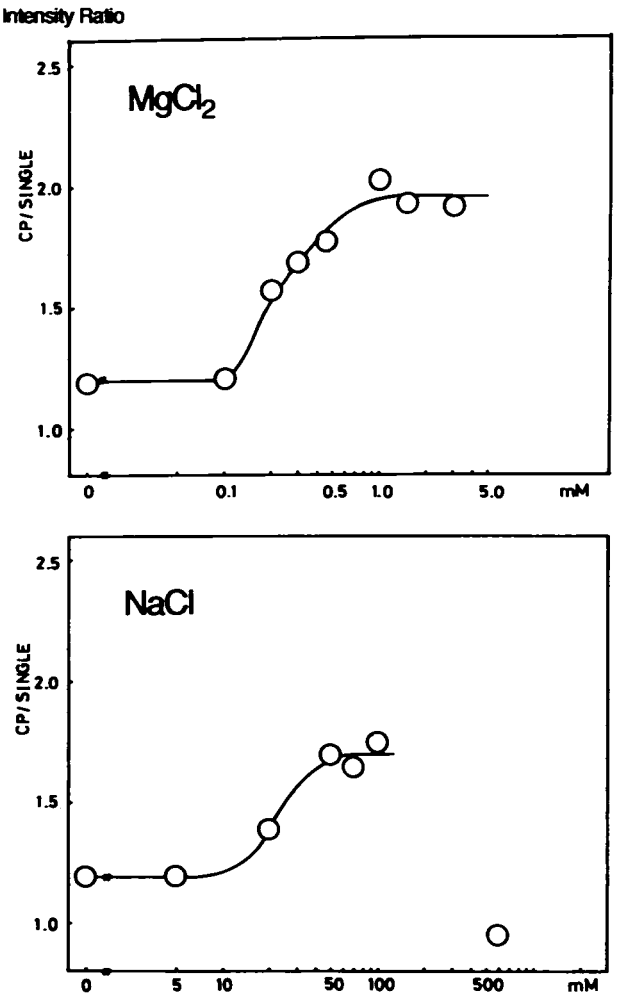

FIGURE 4 Integrated intensity ratio of the cross-polarization and single-pulse powder patterns of the nondigested chromatins as a function of the ion concentration in TE buffer at 4°C. (*Top*) $MgCl_2$; (*bottom*) NaCl.

with that for the formation of the 30-nm filament determined by means of many physicochemical methods, but different from the concentration range just mentioned above (0.1–1.0 mM $MgCl_2$). The wider concentration range for the change in the cross-polarization efficiency suggests that another condensation process follows the formation of the 30-nm filament. In the case of NaCl, the intensity ratio changed from 1.2 to 1.7 in the range of 10–50 mM NaCl as shown in the bottom of Fig. 4. This concentration range well corresponds to that for the chemical shift anisotropy change reported earlier (Nishimoto et al., 1987). In contrast to the case of $MgCl_2$, no further condensation took place. When NaCl concentration was increased to 0.6 M, a symmetric signal appeared instead of the asymmetric powder pattern, and the intensity ratio mentioned above decreased to 0.95, suggesting a loss of the higher order structure. Most of histones H1 and H5 get detached from the DNA at 0.6 M NaCl (van Holde, 1989). Thus, the flexibility of the linker DNA induced by the detachment of histones H1 and H5 can change the powder pattern and the cross-polarization efficiency drastically.

Spin-lattice relaxation time in the rotating frame, and cross-relaxation time of nuclei and chromatins

Cross-polarization efficiency is a function of the cross-relaxation time between phosphorus and protons (T_{HP}), and the spin-lattice relaxation time in the proton rotating frame ($T_{1\rho}$) (Mehring, 1983). The major pathway of the cross-polarization should be the dipole-dipole interactions between the phosphorus and sugar protons of DNA, because the cross-polarization was also observed for the naked DNA in λ phage (Odahara et al., 1994). Therefore, both T_{HP} and $T_{1\rho}$ should be governed by the motion of DNA at a first approximation. The cross-relaxation times of the nuclei and nondigested chromatins at 4°C were obtained by curve-fitting to the contact time dependence of the cross-polarization spectral intensity. They were 0.34 ± 0.02 ms irrespective of the presence of Mg^{2+}. In contrast, the spin-lattice relaxation time in the rotating frame of proton spins ($T_{1\rho}$) was sensitive to the presence of Mg^{2+}. $T_{1\rho}$ was determined by means of the cross-polarization pulse sequence designed for determination of $T_{1\rho}$ (Akutsu, 1986). $T_{1\rho}$ of the nuclei and nondigested chromatins in STM buffer at 4°C were measured at a variety of magnetic fields in the rotating frame (ω_1), and the results are summarized in Table 1. The value of $1/T_{1\rho}$ is plotted as a function of ω_1^2 in Fig. 5 for the nuclei. This field dependence shows that the correlation time of the motion efficient for the relaxation is not in the extremely fast motional regime. The motion of DNA in the chromatins is expected to be aniso-

TABLE 1 Spin-lattice relaxation times in the rotating frame of proton spins ($T_{1\rho}$) of chicken erythrocyte nuclei and nondigested chromatins at a variety of locking fields at 4°C

Sample	$\omega_1 \times 10^{-5}$ (rad/s)	$T_{1\rho}$ (ms)
Nuclei in STM buffer	2.66	4.3
30% sucrose	2.66	4.2
	2.62	4.3
	2.24	3.6
	2.18	3.7
	2.07	3.4
	1.94	3.6
	1.59	3.0
	0.99	2.4
Nuclei in STM buffer	2.53	4.4
0% sucrose	2.38	4.7
	2.24	4.5
	2.18	4.9
Nondigested chromatin in STM buffer	3.20	4.5
30% sucrose	3.14	4.4
	2.71	4.1
	2.38	3.7
	2.34	3.8
	1.91	3.1
	1.87	3.6
	1.40	2.7
	0.92	2.0
Nondigested chromatin in TE buffer	2.49	1.4
30% sucrose	2.38	1.5

STM buffer: 10 mM NaCl, 10 mM Tris, 3 mM $MgCl_2$, pH 7.4; TE buffer: 1 mM Tris, 0.2 mM EDTA, pH 7.4.

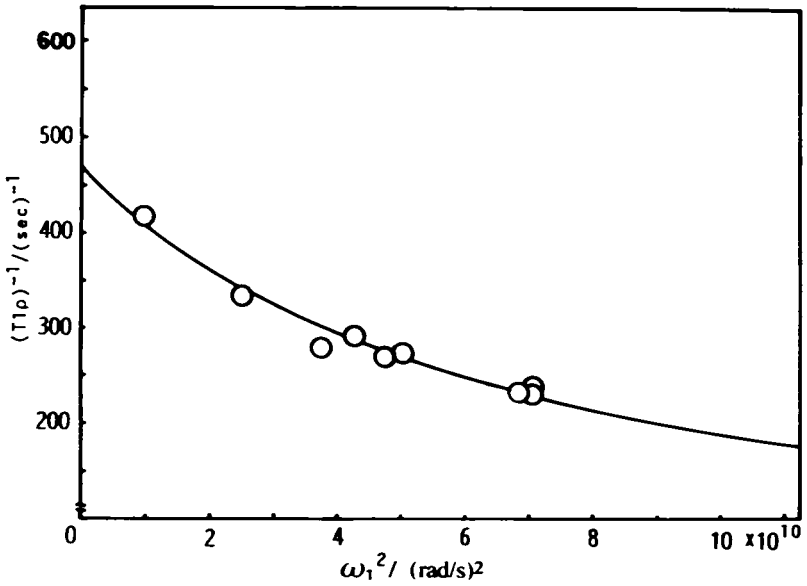

FIGURE 5 Inverse spin-lattice relaxation times in the rotating frame of proton spins of chicken erythrocyte nuclei as a function of the locking field (ω_1). Measurements were carried out for the nuclei in STM buffer with 30% sucrose at 4°C. The solid line is the best-fit curve to Eq. 1.

tropic. But it would be useful to evaluate a rough correlation time by assuming isotropic motions. When the motion of the DNA is assumed to be isotropic, the relaxation time can be described as a function of the correlation time of the motion as follows (Mehring, 1983):

$$\frac{1}{T_{1\rho}} = M_2\tau_c\left\{\frac{1}{1+4\omega_1^2\tau_c^2}+\frac{5}{3}\left(\frac{1}{1+\omega_o^2\tau_c^2}\right)+\frac{2}{3}\left(\frac{1}{1+4\omega_o^2\tau_c^2}\right)\right\}, \quad (1)$$

where ω_0 is the static magnetic field (in rad/s) in the laboratory system and M_2 is the second moment. The correlation time was obtained by least-squares fitting of this equation to the observed data. It was $(1.9 \pm 0.2) \times 10^{-6}$ and $(2.1 \pm 0.2) \times 10^{-6}$ s for the nuclei and nondigested chromatins, respectively. Practically, the correlation time of the DNA motion is identical for the nuclei and nondigested chromatins, as in the case of phosphorus chemical shift anisotropy. In the absence of Mg^{2+}, $T_{1\rho}$ was 1.5 ms at $\omega_1 = 5.7$ rad/s, whereas it was 3.7 ms in the presence of Mg^{2+} (in STM buffer). Sucrose was found to affect $T_{1\rho}$, although it did not affect the chemical shift anisotropy. The value of $T_{1\rho}$ in the absence of sucrose was greater (4.7 ms at $\omega_1 = 5.7$ rad/s for the nuclei in STM buffer) than that in the presence of 30% sucrose. As shown in Table 1, the relaxation time did not show the field dependence in the absence of sucrose, suggesting that the motional correlation time is in the fast motional regime.

Phosphorus NMR spectra of digested chromatins, H1,H5-depleted chromatins and nucleosome cores

Because extensive physicochemical studies have been carried out on the digested (or soluble) chromatins and nucleosome cores, we examined these systems as well. In these cases, we worked on pellets, as mentioned under Materials and Methods. Phosphorus NMR spectra of the soluble chromatins in TE buffer and [TE + 3 mM $MgCl_2$] buffer, and H1,H5-depleted chromatins in [TE + 3 mM $MgCl_2$] buffer at 4°C showed partially averaged asymmetric powder pattern similar to Fig. 4 *A*. Their phosphorus chemical shift anisotropies and $T_{1\rho}$ are summarized in Table 2. The chemical shift anisotropies of the digested chromatins in the presence and absence of 3 mM $MgCl_2$ were more or less similar, suggesting that the motion of the nucleosomes was suppressed by the high density of the digested chromatins in the pellet. The chemical shift anisotropy of the digested chromatins in the presence of 3 mM $MgCl_2$ was identical with those of the nuclei and nondigested chromatins in STM buffer. In contrast to the chemical shift anisotropy, their spin-lattice relaxation times in the proton rotating frame were different from each other. The chemical shift anisotropy of the H1,H5-depleted chromatins was smaller in absolute value than those of the digested chromatins with and without $MgCl_2$, suggesting that even in the pellet, they cannot be so closely packed as the digested chromatins. Although the qualitative order of the chemical shift anisotropy for the digested and H1,H5-depleted chromatins was the same as that for the

TABLE 2 Phosphorus chemical shift anisotropies and spin-lattice relaxation times in the rotating frame of the digested chromatins and nucleosome cores at 4°C

Sample	Chemical shift anisotropy (ppm)	$T_{1\rho}$ (ms)
Soluble chromatin (0 mM $MgCl_2$)	−152	2.6 (2.49)*
Soluble chromatin (3 mM $MgCl_2$)	−156	5.2 (2.75)*
H1,H5-depleted chromatin (3 mM $MgCl_2$)	−145	
Nucleosome core (0 mM $MgCl_2$)	−159	

* The value in the parentheses is the locking field in rad/s.

counterparts of the nondigested chromatins, the quantitative difference was much more significant for the latters.

A phosphorus NMR spectrum of the nucleosome cores obtained by the cross-polarization method at 4°C also showed a partially averaged asymmetric powder pattern as shown in Fig. 3 D. The chemical shift anisotropy was −159 ppm. This absolute value is a little larger than those of the nondigested chromatins in the presence of 3 mM $MgCl_2$ and the soluble chromatin pellet at 4°C. This suggests that the upper limit of the chemical shift anisotropy of the chromatins is determined by that of the nucleosome cores. The chemical shift anisotropy is further averaged by the motion of the nucleosome core itself, which would be caused by the flexibility of the linker DNA. The value of −159 ppm can be regarded as the intrinsic chemical shift anisotropy of the nucleosomes.

DISCUSSION

The dynamic properties of the higher order structure of the chromatins have been investigated in this work using intact cells, nuclei, nondigested chromatins, and digested chromatins. The nondigested chromatins allowed us to perform in vitro investigation of the higher order structure with an intact system under the same conditions as the soluble (digested) chromatins were investigated. Thus, we can compare the results directly with the accumulated data for the soluble (digested) chromatins. Because the observed NMR parameters (the spectral pattern, chemical shift anisotropy, temperature dependence of the chemical shift anisotropy and the spin-lattice relaxation times in the rotating frame) are identical for the nondigested chromatins and nuclei, the higher order structure observed for the nondigested chromatins would be identical with that in the nuclei as far as the local structure is concerned. Therefore, this chemical shift anisotropy (−156 ppm at 4°C) should represent the basic higher order structure characterized in the digested (soluble) chromatins.

The chemical shift anisotropy of the nucleosome cores was found to be −159 ppm. This shows that the nucleosomal DNA still interacts strongly with the histone octamer even though histones H1 and H5 are removed. It has been reported that the interaction is retained in the presence of salt up to 1 M (Bashkin et al., 1993). The chemical shift anisotropy of the nucleosome cores is close to that of T4 phage (Akutsu et al., 1980), in which naked DNA rods are closely packed (Earnshaw and Casjens, 1980). Because the anisotropy of dry DNA is −220 ppm (Odahara et al., 1994), the nucleosomal DNA is still flexible to a certain extent despite the strong DNA-histone octamer interactions. This would be the inherent nature of B-form DNA. Because large scale motions in the rotation and bending would be suppressed to a great extent in the nucleosome cores, rapid local fluctuations of restricted amplitude must average the chemical shift tensor. Structural fluctuation between B_I and B_{II} conformations was suggested for the origin of the structural flexibility of DNA in solution (Nikonowicz and Gorenstein, 1990). This might partly contribute to the rapid local fluctuation. In the nuclei and nondigested chromatins, further averaging of the chemical shift tensor takes place through the fluctuation of the nucleosomes, which is induced by the motion of the linker DNA. The effect of the linker DNA motion was dramatically shown on the addition of 0.6 M NaCl which removes histones H1 and H5 from the linker DNA. In this sense, histones H1 and H5 are key proteins in regulating dynamic structure of the chromatins.

Because the chromatins are composed of nucleosome cores and linker DNA. A ^{31}P-NMR spectrum should be contributed from two major parts. The spectra of the chromatins in the presence of Mg^{2+}, however, have not shown a clear indication for overlapping of two components. This suggests that the histones H1 and H5 suppress the motional amplitude of nucleosome cores and linker DNA in a similar way through formation of a tight complex of the two parts in the 30-nm filament. The chemical shift of the nondigested chromatins in TE buffer (in the absence of Mg^{2+}) is more averaged, and their spectrum is not a typical one-component powder pattern, suggesting that the linker DNA in the 10-nm filament is more flexible than that in the 30-nm filament. This flexibility could play an important role in the initiation of transcription because it would allow other molecules to access histones.

Judging from the correlation time, the motions efficient for the spin-lattice relaxation in the rotating frame of proton spins of the nuclei and nondigested chromatins must be segmental fluctuations of DNA (Fujiwara and Shindo, 1985). Because segmental motions in the nucleosome cores are almost completely suppressed, the most efficient relaxation site for $T_{1\rho}$ should be localized in the linker DNA region. The single exponential property of the observed relaxation shows that the proton spins in the nucleosome cores and linkers have the same relaxation time through spin diffusion. On the basis of this model, $T_{1\rho}$ of different samples can be elucidated reasonably. The increase in $T_{1\rho}$ of the nondigested chromatins with the introduction of Mg^{2+} in the presence of 30% sucrose can be attributed to the suppression of the motions of the linker DNA on the formation of the 30-nm filament, with the motional correlation time being in the slow motional regime. Although the chemical shift anisotropies of the digested chromatins in the presence and absence of Mg^{2+} were very close to each other, $T_{1\rho}$ were quite different for these two samples. This apparent inconsistency can be explained as follows. Although the motional amplitudes of the nucleosome core and linker DNA are suppressed to a more or less similar extent by the close packing in the pellet for the 30- and 10-nm filaments, the rate of the motion of their linker DNA still reflects the difference in their ordered structures.

It was suggested that Na^+ and Mg^{2+} would play different roles in the organization of a higher order structure. Because the phosphorus chemical shift anisotropy was different for the 30-nm filaments induced by Na^+ and Mg^{2+} (−150 and −156 ppm at 4°C, respectively), the rigidity must be different in these two types of 30-nm filaments (Nishimoto et al., 1987). After the formation of the 30-nm filament, a

further increase in the cross-polarization efficiency was observed on increasing the Mg^{2+} concentration from 0.3 to 1.0 mM in this work. Cross-polarization efficiency is a function of the cross-relaxation time (T_{HP}) and $T_{1\rho}$ (Mehring, 1983). Because the cross-relaxation time was constant at all Mg^{2+} concentrations examined, the increase in the cross-polarization efficiency can be attributed to an increase in $T_{1\rho}$. Because the correlation time of the motion was shown to be in the slow motional regime, further suppression of motions of the linker DNA in this Mg^{2+} concentration range is suggested. The suppression of the linker DNA motions must be the consequence of a further compaction of the chromatins. This compaction can be ascribed to the side-by-side packing of the 30-nm filaments, because electron microscopy and x-ray studies have shown that when Mg^{2+} is removed, the 30-nm filament remains intact, but the chromatin is dispersed (Thoma et al., 1979; Langmore and Paulson, 1983). A polarized photo-bleaching investigation on mudpuppy nuclei showed that although an aggregated structure of chromatins is formed in the presence of 3mM $MgCl_2$ with the physiological monovalent salt concentration (~90 mM), it is lost in the absence of magnesium ion (Selvin et al., 1990). The aggregated structure was also explained as side-by-side compaction of 30-nm filament. Our results showed that such compaction suppresses the rate of the linker DNA motions but does not affect the amplitude of the fluctuation of the nucleosomes significantly. The latter is natural, because the chemical shift anisotropy of the 30-nm filament is already close to the intrinsic value for the nucleosomes. If the linker DNA is localized in the center of the 30-nm filament, as suggested by Butler (1984), $T_{1\rho}$ would not be affected by the compaction. Thus, the linker DNA region should be located in the vicinity of the surface of the 30-nm filaments. The conclusion is consistent with the observations as to the nuclease sensitivity of the linker DNA and protease sensitivity of the H1 histone (van Holde, 1989).

In conclusion, our results have shown that histones H1 and H5 are the key proteins for the regulation of the dynamic structure of the chromatins. The regulation is controlled through interactions with other molecules such as Na^+ and Mg^{2+}. If the linker DNA regions together with histones H1 and H5 are located on the surface of the 30-nm filament, it would be much easier to change the biologically inactive higher order structure to more active structure through the specific interaction of some messenger molecules with the histones H1 and/or H5. Higher sensitivity of the histones H1 and H5 to the salt concentration than the core histones also suggests their active roles in regulation of the functions of the nucleosomes. Temperature change of the higher order structure of the chromatins observed in Fig. 2 implies that the chromatins are ready for the change even in the most rigid and stable structure.

This work was partly supported by a grant-in-aid from the Ministry of Education, Science and Culture (No. 05101004), and Special Coordination Funds of the Science and Technology Agency of the Japanese government.

REFERENCES

Akutsu, H. 1986. Detection of slow motional changes in the phosphatidylcholine bilayers by ^1H-^{31}P cross polarization dynamics. *J. Magn. Reson.* 66:250–263.

Akutsu, H., H. Satake, and R. M. Franklin. 1980. Phosphorus nuclear magnetic resonance studies on the lipid-containing bacteriophage PM2. *Biochemistry.* 19:5264–5270.

Ashikawa, I., K. Kinoshita, Jr., A. Ikegami, Y. Nishimura, and M. Tsuboi. 1985. Increased stability of the higher order structure of chicken erythrocyte chromatin: nanosecond anisotropy studies of intercalated ethidium. *Biochemistry.* 24:1291–1297.

Bashkin, J., J. J. Hayes, T. D. Tullius, and A. P. Wolffe. 1993. Structure of DNA in a nucleosome core at high salt concentration and at high temperature. *Biochemistry.* 32:1895–1898.

Bordas, J., L. Perez-Grau, M. H. J. Koch, M. C. Vega, and C. Nave. 1986. The superstructure of chromatin and its condensation mechanism II. Theoretical analysis of the x-ray scattering patterns and model calculations. *Eur. J. Biophys.* 13:175–185.

Butler, P. J. M. 1984. A defined structure of the 30 nm chromatin fibre which accommodates different nucleosomal repeat lengths. *EMBO J.* 3: 2599–2604.

Cavazza, B., G. Brizzolara, G. Lazzarini, E. Patrone, M. Piccardo, P. Barboro, S. Parodi, A. Pasini, and C. Balbi. 1991. Thermodynamics of condensation of nuclear chromatin. A differential scanning calorimetry study of the salt-dependent structural transitions. *Biochemistry.* 30:9060–9072.

Earnshaw, W. C., and S. R. Casjens. 1980. DNA packaging by the double-stranded DNA bacteriophages. *Cell.* 21:319–331.

Finch, J. T., and A. Klug. 1976. Solenoidal model for superstructure in chromatin. *Proc. Natl. Acad. Sci. USA.* 73:1897–1901.

Fujiwara, T., and H. Shindo. 1985. Phosphorus-31 nuclear magnetic resonance of highly oriented DNA fibers. 2. Molecular motions in hydrated DNA. *Biochemistry.* 24:896–902.

Hansen, J. C., K. E. van Holde, and D. Lohr. 1991. The mechanism of nucleosome assembly onto oligomers of the sea urchin 5S DNA positioning sequence. *J. Biol. Chem.* 266:4276–4282.

Hansen, J. C., and J. Ausio. 1992. Chromatin dynamics and the modulation of genetic activity. *Trends Biochem.* 17:187–191.

Hayes, J. J., and A. P. Wolffe. 1992. Histones H2A/H2B inhibit the interaction of transcription factor IIIA with the *Xenopus borealis* somatic 5s RNA gene in a nucleosome. *Proc. Natl. Acad. Sci. USA* 89:1229–1233.

Laemmli, U. K. 1970. Cleavage of structural proteins during the assembly of the head of bacteriophage T4. *Nature.* 227:680–685.

Langmore, J. P., and J. R. Paulson. 1983. Low angle X-ray diffraction studies of chromatin structure in vivo and in isolated nuclei and metaphase chromosomes. *J. Cell Biol.* 96:1120–1131.

Makarov, V., S. Dimitrov, V. Smirnov, and I. Pashev. 1985. A triple helix model for the structure of chromatin fiber. *FEBS Lett.* 181:357–361.

McGhee, J. D., J. M. Nickol, G. Felsenfeld, and D. C. Rau. 1983. Higher order structure of chromatin: orientation of nucleosomes within the 30 nm chromatin solenoid is independent of species and spacer length. *Cell.* 33:831–841.

Mehring, M. 1983. Principles of High Resolution NMR in Solids. 2nd Ed. Springer-Verlag, Berlin.

Nikonowicz, E. P., and D. G. Gorenstein. 1990. Two-dimensional ^1H and ^{31}P NMR spectra and restrained molecular dynamics structure of a mismatched GA decamer oligodeoxyribonucleotide duplex. *Biochemistry.* 29:8845–8858.

Nishimoto, S., H. Akutsu, and Y. Kyogoku. 1987. The presence of the 30 nm filament structure of chromatins in intact chicken erythrocytes observed by ^{31}P NMR. *FEBS Lett.* 213:293–296.

Odahara, T., S. Nishimoto, N. Katsutani, Y. Kyogoku, Y. Morimoto, A. Matsushiro, and H. Akutsu. 1994. Dynamic properties of nucleic acids in biosupramolecular systems as studied by ^{31}P NMR. *J. Biochem.* 115: 270–278.

Ramakrishnan, V., J. T. Finch, V. Graziano, P. L. Lee, and R. M. Sweet. 1993. Crystal structure of globular domain of histone H5 and its implications for nucleosome binding. *Nature.* 362:219–223.

Richmond, T. J., J. T. Finch, B. Rushton, D. Rohdes, and A. Klug. 1984. Structure of the nucleosome core particle at 7 A resolution. *Nature.* 311: 532–537.

Selvin, P. R., B. A. Scalettar, J. P. Langmore, D. Axelrod, M. P. Klein, and J. E. Hearst. 1990. A polarized photobleaching study of chromatin reorientation in intact nuclei. *J. Mol. Biol.* 214:911–922.

Staynov, D. Z. 1983. Possible nucleosome arrangements in the higher-order structure of chromatin. *Int. J. Biol. Macromol.* 5:3–9.

Stejskal, E. O., J. Schaefer, M. D. Sefcik, and R. A. McKay. 1981. Magic-angle carbon-13 nuclear magnetic resonance study of the compatibility of solid polymeric blends. *Macromolecules.* 14:275–279.

Thoma, F., T. Koller, and A. Klug. 1979. Involvement of histone H1 in the organization of the nucleosome and of the salt-dependent superstructures of chromatin. *J. Cell Biol.* 83:403–427.

van Holde, K. E. 1989. Chromatin. Springer-Verlag, New York.

van Holde, K. E. 1993. The omnipotent nucleosome. *Nature.* 362: 111–112.

Widom, J., J. T. Finch, and J. O. Thomas. 1985. Higher-order structure of long repeat chromatin. *EMBO J.* 4:3189–3194.

Williams, S. P., B. D. Athey, L. J. Muglia, R. S. Schappe, A. H. Gough, and J. P. Langmore. 1986. Chromatin fibers are left-handed double helices with diameter and mass per unit length that depend on linker length. *Biophys. J.* 49:233–248.

Williams, S. P., and J. P. Langmore. 1991. Small angle x-ray scattering of chromatin. Radius and mass per unit length depend on linker length. *Biophys. J.* 59:606–618.

Woodcock, C. L. F., L.-L. Y. Frado, and J. B. Rattner. 1984. The higher order structure of chromatin: evidence for a helical ribbon arrangement. *J. Cell Bio.* 99:42–52.

Worcel, A., S. Strogatz, and D. Riley. 1981. Structure of chromatin and the linking number of DNA. *Proc. Natl. Acad. Sci. USA.* 78:1461–1465.

Zentgraf, H., B. Deumling, E. D. Jarusch, and W. W. Franke. 1971. Nuclear membranes and plasma membranes from hen erythrocytes. *J. Biol. Chem.* 246:2986–2995.